Carbohydrate Polymers 86 (2011) 806–811

Contents lists available at ScienceDirect

Carbohydrate Polymers

journal homepage: www.elsevier.com/locate/carbpol

Preparation, structure and BMP-2 controlled release of heparin-conjugated hyaluronan microgels

Jianhao Zhao[a,b,*], Chunhong Luo[a], Yuqi Chen[a], Dan Wu[a], Chaoxuan Shen[a], Wanqing Han[a], Mei Tu[a,b], Rong Zeng[a,b]

[a] Department of Materials Science and Engineering, College of Science and Engineering, Jinan University, Guangzhou 510632, China
[b] Engineering Research Center of Artificial Organs and Materials, Ministry of Education, Guangzhou 510632, China

ARTICLE INFO

Article history:
Received 29 January 2011
Received in revised form 11 May 2011
Accepted 18 May 2011
Available online 26 May 2011

Keywords:
Heparin
Hyaluronan
Microgel
Controlled release
Growth factors

ABSTRACT

Heparin-conjugated hyaluronan (HA-Hp) microgels with different heparin content, i.e., 1%, 5% and 10% (w/w), were synthesized by an inverse emulsion polymerization technique for the controlled release of bone morphogenetic protein-2 (BMP-2). A heparin conjugation percentage of about 90% was obtained by elemental analysis. Hyaluronan microgels showed a smooth surface and dense network, whereas HA-Hp microgels exhibited a rougher surface with holes and concaves, and a looser internal structure with increasing the heparin content instead. However, the major microgel size of about 3 μm was independent of the heparin amount. Among the samples, HA-Hp-10% microgels existed the highest equilibrium swelling ratio of 11.8 due to its least cross-linking network. A higher BMP-2 loading efficiency and a slower release profile with increasing the heparin content indicated the conjugated heparin in HA-Hp microgels was in favor of BMP-2 binding and the sustained delivery maybe attributed to the electrostatic interaction between heparin and BMP-2.

1. Introduction

Growth factors (GFs) play a crucial role in the communication and information transfer between cells and their microenvironment. However, the short half-lives of GFs in human body make it necessary to realize the controllable and long-term delivery for tissue engineering (Tayalia & Mooney, 2009). Even though a variety of delivery systems have been developed, such as microcapsules, fibers, grafts and hydrogels (Chen et al., 2006; Edelman, Nugent, Smith, & Karnovsky, 1992; Liao, Wan, Yim, & Leong, 2005; Nakamura et al., 2007; Zeng et al., 2009), the controlled release of GFs is still a challenge in tissue engineering and regenerative medicine.

Polysaccharide-based microgels/nanogels, such as chitosan, hyaluronan (HA), chondroitin sulfate, cellulose and alginate have recently attracted a great deal of interest in tissue engineering and drug delivery since they have high water content, functionality, biocompatibility, tunable size from submicrons to tens of nanometers, large surface area for multivalent bioconjugation, and interior network for the incorporation of therapeutics as well as their exciting properties of biodegradation, abundance in nature, nontoxicity and low cost (Oh, Lee, & Park, 2009; Yang & Kim, 2010; Zhao et al., 2011). Especially, HA, a linear polysaccharide of alternating D-glucuronic acid and *N*-acetyl-D-glucosamine, is found natively in many tissues and plays a role in cellular response, which is considered to be one of the most popular polysaccharide-based hydrogel matrices in tissue engineering (Jiang, Liang, & Noble, 2007; Sahoo, Chung, Khetan, & Burdick, 2008; Toole, 2001).

However, a simple physical entrapment of GFs within HA particles will lead to the uncontrolled short-term release profile (Zavan et al., 2009). Recently, it has been shown that secondary association immobilization via electrostatic attractions between an intermediate group, e.g., heparin or a proteolytically active peptide, and GF can control the release profile (Tayalia & Mooney, 2009). Heparin, a highly sulfated glycosaminoglycan, has high affinity for basic GFs via primarily electrostatic interactions between N- and O-sulfated residues of heparin and the lysine and arginine residues of GFs (Godspodarowicz & Cheng, 1986; Wissink et al., 2000). Several approaches have been used to investigate the controlled release of GFs by heparin-functionalized biomaterials. For example, heparin-entrapped HA hydrogels could slow the release of human vascular endothelial growth factor (VEGF), but there was no obvious difference in the VEGF release profile when increasing the heparin content from 0.3% (w/w) to 3% (w/w) (Pike et al., 2006). Heparin has also been used to sustain the delivery of avidin and PDGF-bb from alginate/heparin polyelectrolyte complex fibers at a certain pH

* Corresponding author at: Department of Materials Science and Engineering, College of Science and Engineering, Jinan University, Guangzhou 510632, China. Tel.: +86 20 85223271; fax: +86 20 85223271.
E-mail address: jhzhao@jnu.edu.cn (J. Zhao).

0144-8617/$ – see front matter © 2011 Elsevier Ltd. All rights reserved.
doi:10.1016/j.carbpol.2011.05.026

value, where the release profiles was significantly influenced by the complex charges (Liao et al., 2005). Recently, heparin-conjugated chitosan–alginate scaffolds has been used to control the delivery of basic fibroblast growth factor (bFGF) and found that the rate of bFGF release from the scaffold decreased in a controlled manner with increasing the heparin concentration (Ho, Mi, Sung, & Kuo, 2009). Hereby, it can be hypothesized that no matter freely entrapped or formed polyelectrolyte complex with the matrix, heparin is feasible to diffuse outside from the matrix due to concentration difference, and pH or charge changes, and subsequently decrease the regulating efficiency of GFs release. In contrast, conjugation is a more efficient way for heparin immobilization into the matrix. However, there has been no report of heparin-conjugated hyaluronan (HA-Hp) microgels being designed as a carrier for the GFs controlled release studies.

Bone morphogenetic protein-2 (BMP-2), a growth factor that induces the differentiation of mesenchymal stem cells into chondrocytes, and influences the cartilage formation, has been extensively used in tissue engineering (Goldring, Tsuchimochi, & Ijiri, 2006; Hall & Miyake, 2000; Krawczak, Westendorf, Carlson, & Lewis, 2009; Maeda, Sano, & Fujioka, 2004). However, BMP-2 has not been fully used in clinics due to its short *in vivo* half-life and susceptibility to degradation in a soluble form (Babensee, McIntire, & Mikos, 2000; Nimni, 1997). Hence, a delivery system releasing BMP-2 in a controlled manner would maximize its application in tissue regeneration. In this work, a series of HA-Hp microgels with different heparin content were synthesized and used as the carriers for BMP-2 delivery. The electrostatic interactions between basic heparin-binding domain on BMP-2 and acidic sulfate groups on heparin were designed to realize the immobilization and controlled release of BMP-2. The effects of heparin content on the particle size, and surface and internal structure of HA-Hp microgels were investigated by dynamic laser scattering (DLS), scanning electron micrograph (SEM) and transmission electron microscope (TEM) respectively. Finally, the loading efficiency and release profiles of BMP-2 in HA-Hp microgels were studied and discussed by an enzyme-linked immunosorbent assay (ELISA).

2. Materials and methods

2.1. Materials

Sodium hyaluronan (M_w, 450 kDa) was provided by Shandong Institute of Medical Instruments. Sodium heparin (M_w, 15 kDa), diocetyl sulfosuccinate sodium salt (AOT, 98%), 2,2,4-trimethylpentane (isooctane, anhydrous), divinyl sulfone (DVS), and 1-heptanol (1-HP) were purchased from Aldrich–Sigma. All other reagents and solvents used were analytical grade.

2.2. Synthesis of HA-Hp microgels

HA-Hp microgels were synthesized using an AOT/isooctane/water inverse microemulsion cross-linking system (Jha et al., 2009). Briefly, 4 mg/mL HA and 4 mg/mL heparin solutions were prepared by dissolving a certain weight of HA and heparin in 0.2 M sodium hydroxide solution respectively. The organic phase was composed of 0.2 M AOT and 0.04 M 1-HP in isooctane. 0.27 mL mixture of HA and heparin solution with an heparin content of 1%, 5% and 10% (w/w) respectively was vortex mixed with 7.5 mL AOT/1-HP/isooctane solution in a 20 mL vial. DVS (0.4 μL) was subsequently added to the system and vortex mixed again to get dispersed. Then, the reaction proceeded for 30 min at room temperature under vigorous stirring. After precipitating the microemulsion in a large excess of acetone, the particles were collected by centrifugation and washed with water, ethanol and acetone for several times respectively. HA-Hp microgels with different heparin content were obtained after being dried under vacuum at room temperature. Yield: 80%. HA microgel without heparin component was used as the control.

2.3. Characterizations

The heparin content in HA-Hp microgels was measured using an Elemental Analyzer (Vario EL Elementar, Germany). The actual heparin percentage in HA-Hp microgels was calculated based on the ratio of the sulfur element percentage in HA-Hp microgels and heparin. The heparin conjugation percentage was obtained by comparing the actual and feed content of heparin in HA-Hp microgels.

The average particle size and distribution of HA-Hp microgels dispersed in distilled water was measured by DLS using a Laser Diffraction Particle Size Analyzer (LS 230, Beckman Coulter, USA).

The morphologies of HA-Hp microgels were observed by SEM (PHILIPSXL-30 ESEM) and TEM (PHILIPS, TECNAI-10, NETHERLANDS). Before SEM analysis, a gold layer was coated on the specimen surface in a sputter coater (BAL-TEC, SCD005).

The swelling ratio of HA-Hp microgels was measured gravimetrically. Briefly, the dry microgel samples were placed in a vial with known weight, and the dry weight of microgels was determined. After the dry microgels were soaked in phosphate-buffered saline solution (PBS, pH 7.4) at 37 °C for 1 h, the supernatant was removed by centrifugation at 4500 rpm for 10 min. The wet weight of microgels was subsequently measured. The equilibrium swelling ratio was obtained as the ratio of the wet weight to the dry weight.

BMP-2 loading and release studies of HA-Hp microgels were performed as follows: 1.0 mg HA-Hp microgels were soaked in 200 μL binding buffer [0.1% (v/v) BSA, 1% (v/v) Penicillin–Streptomycin (PS), 0.1 mM phenylmethylsulfonyl fluoride (PMSF) in PBS] containing 200 ng BMP-2 for 2 h at room temperature. To measure the loading efficiency, the unloaded BMP-2 in the supernatant was collected and quantified. Subsequently, the medium was refreshed with 400 μL PBS containing 100 U/mL PS and incubated at 37 °C. The supernatant was collected and the medium was refreshed at the designed time intervals during incubation for 15 days. The amount of BMP-2 in the release medium was determined by ELISA assay.

3. Results and discussion

3.1. Synthesis of HA-Hp microgels

It has been reported that HA hydrogel particle can been synthesized using DVS as the cross-linker in an inverse microemulsion polymerization system, where DVS reacted with the OH group of hydroxymethylene on *N*-acetyl-D-glucosamine unit of HA via Michael addition under basic conditions (Hahn, Jelacic, Maier, Stayton, & Hoffman, 2004; Rizzi et al., 2006). There also exist some *N*-acetyl-D-glucosamine units in the heparin molecular chain. Herein, it is hypothesized that HA-Hp microgel can also be prepared by using the similar system of HA hydrogel particle preparation. The synthesis and molecular structure of HA-Hp microgel by an inverse emulsion polymerization technique were shown in Scheme 1. Since the amount of heparin played a key role on the binding and release of GFs (Pike et al., 2006), various heparin content, i.e. 1%, 5% and 10% (w/w) were used to prepare HA-Hp microgels in this work. The heparin conjugation not only can endow the BMP-2 binding function to HA microgels, but also can realize the sustained release of BMP-2 via HA-Hp microgel delivery system.

3.2. Heparin content and conjugation percentage

For HA-Hp microgels, the amount of heparin will have a major effect on BMP-2 loading and the release profile, which can be quan-

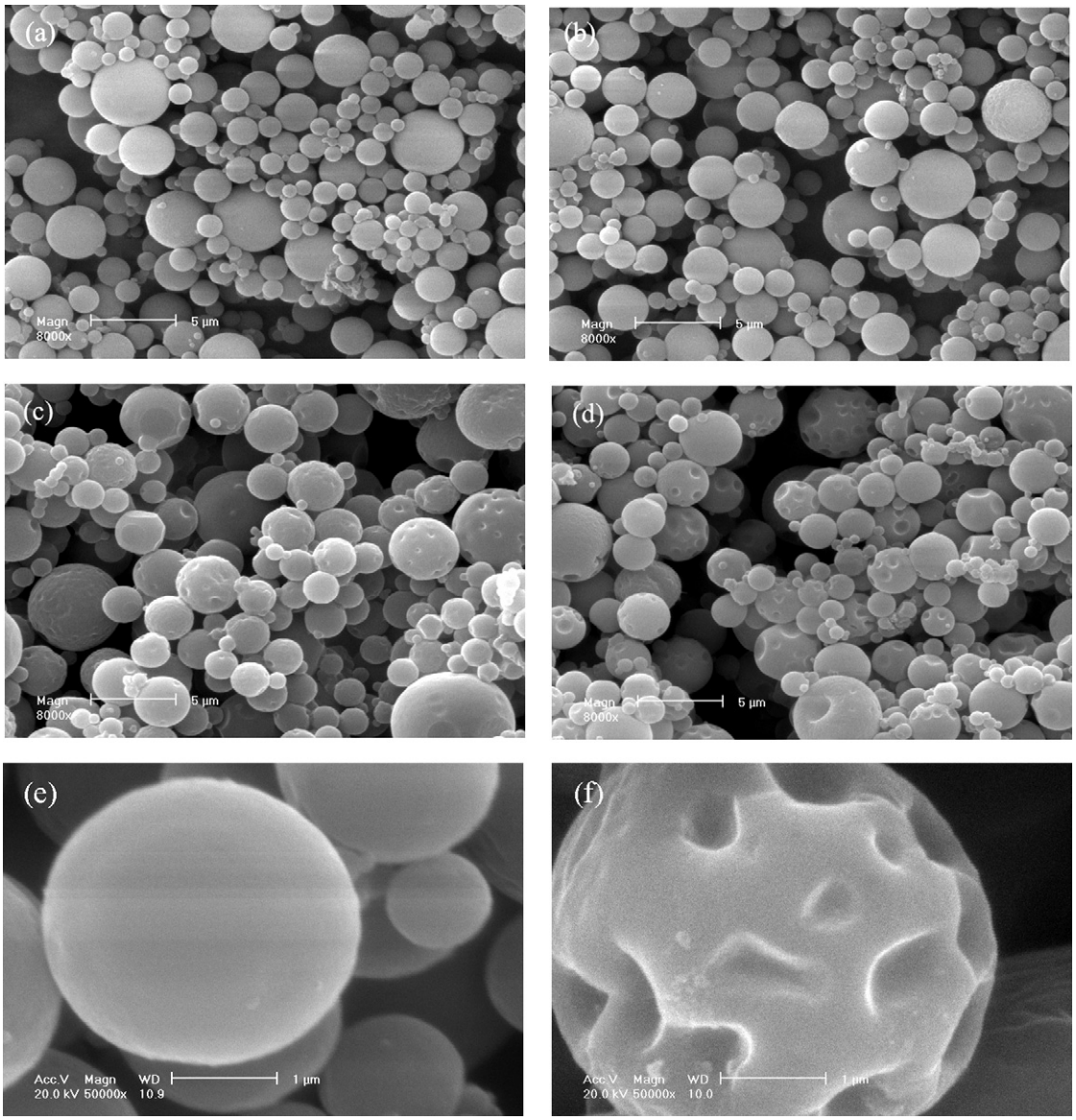

Fig. 1. SEM images of HA and HA-Hp microgels with different Hp content. (a) HA; (b) HA-Hp-1%; (c) HA-Hp-5%; (d) HA-Hp-10%; (e) enlargement of (a); and (f) enlargement of (d).

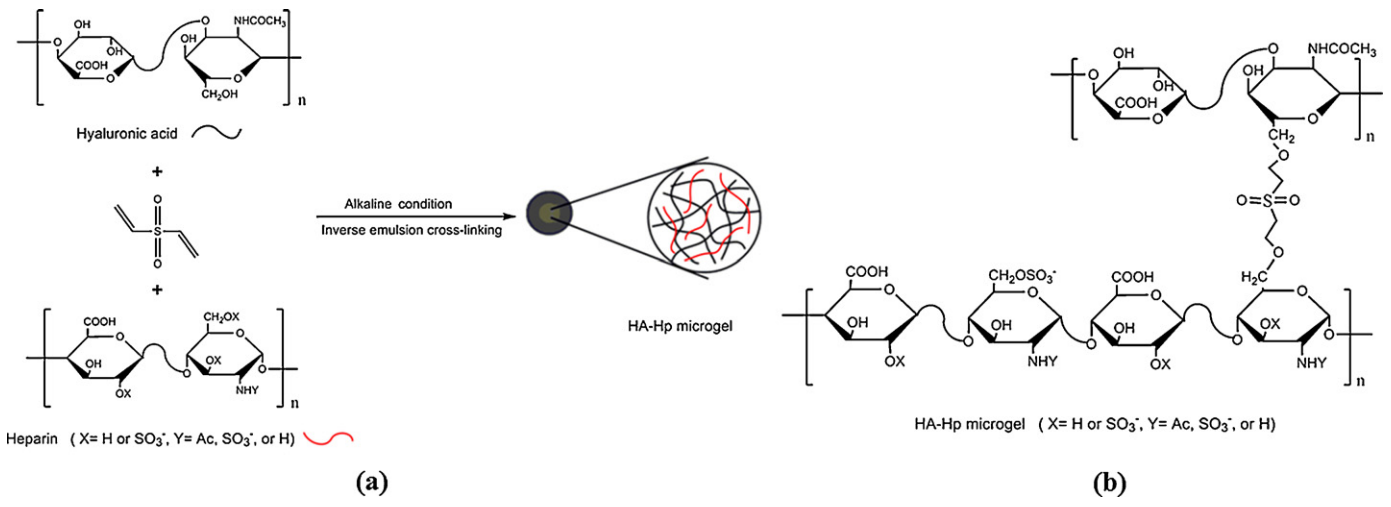

Scheme 1. Synthesis and molecular structure of HA-Hp microgels by an inverse emulsion polymerization technique. (a) Synthesis of HA-Hp microgels and (b) molecular structure of HA-Hp microgels.

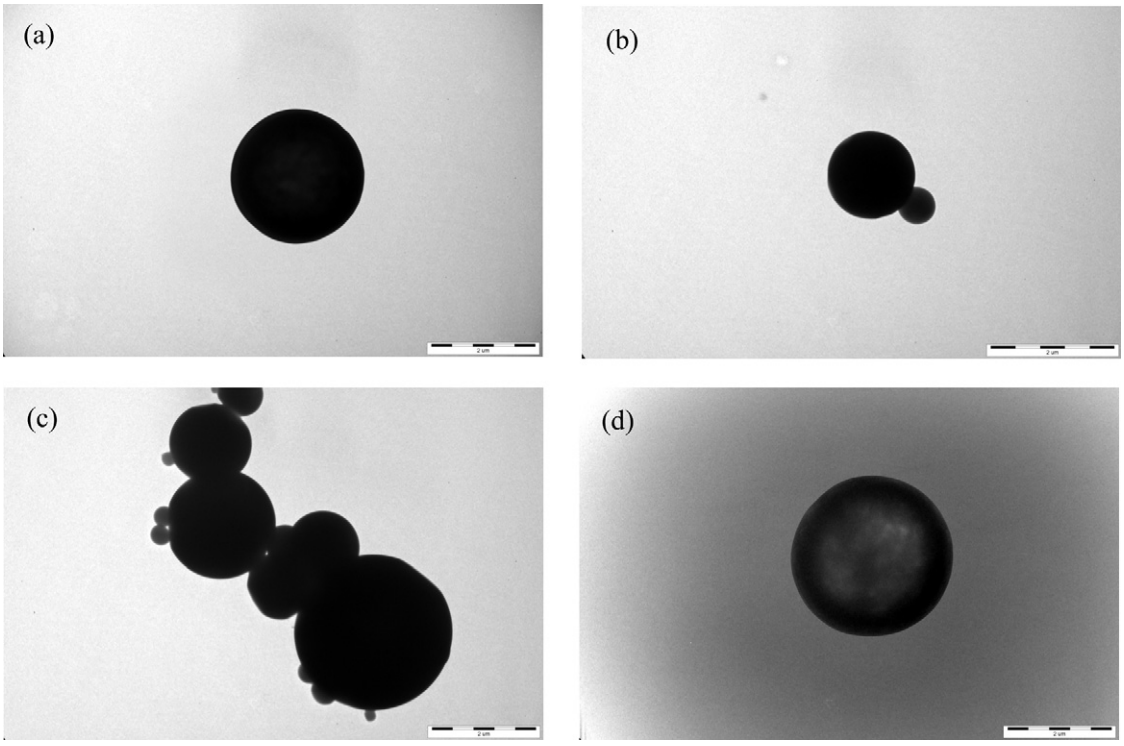

Fig. 2. TEM images of HA and HA-Hp microgels with different Hp content. (a) HA; (b) HA-Hp-1%; (c) HA-Hp-5%; (d) HA-Hp-10%.

tified by elemental analysis. The percentages of carbon, hydrogen and sulfur elements in heparin and HA-Hp microgels were respectively measured, as shown in Table 1. Since the sulfur element in HA-Hp microgels was only from heparin, the actual heparin content in HA-Hp-1%, HA-Hp-5% and HA-Hp-10% microgels could be calculated to be 0.9 wt%, 4.2 wt% and 8.6 wt% respectively by the ratio of sulfur element percentage in HA-Hp microgels and heparin. Correspondingly, the heparin conjugation percentages for these three HA-Hp microgels were evaluated to be 90%, 92% and 89% respectively based on the actual and feed content of heparin in HA-Hp microgels. The results showed that heparin was efficiently conjugated to hyaluronan molecular chains for all samples using this inverse microemulsion polymerization system.

3.3. Morphological analysis

Fig. 1 shows the SEM images of HA-Hp microgels with different heparin content. Well-defined spherical particles with relatively narrow size distribution for all samples were generated. A smooth surface of HA microgels was seen (Fig. 1a and e), whereas a rougher surface was obtained with increasing the heparin content. At 5% (w/w) and 10% (w/w) of heparin, some small holes and concaves occurred on the particle surface (Fig. 1c, d and f). It is possible that with the increase of heparin percentage, more defects and looser cross-linking structure were formed on the zone of HA and heparin cross-linking reaction because the molecule chain length of heparin was much shorter than that of HA. These defects should be responsible for the formation of small holes on the surface of HA-Hp microgels, and the loose cross-linking structure maybe led to the formation of concaves by the mutual pack and compression of microgels (Lou, Vijayasekaran, Sugiharti, & Robertson, 2005). This hypothesis was further confirmed by the TEM images of HA and HA-Hp microgels in Fig. 2. HA microgels showed a round and dense appearance. In contrast, HA-Hp microgels exhibited a more irregular surface and a somewhat looser interior structure with the grey regions on the surface (Fig. 2b and c). Especially, when the heparin content was enhanced to be 10% (w/w), a loose internal structure was obviously observed (Fig. 2d), which should be ascribed to the lowest cross-linking density of HA-Hp-10% microgels among all these microgels samples. Therefore, these less cross-linking HA-Hp microgels were feasible to generate concaves on the surface after being packed and compressed with each other.

3.4. Particles size and distribution

The particle size and distribution of HA and HA-Hp microgels were characterized by DLS analysis, as shown in Fig. 3. Most of the microgels were distributed in the range of 2–5 μm with an average particle size of about 3 μm, which was little affected by the heparin content. There also existed a minor percentage of particles with a smaller size at about 100–200 nm. The presence of two-particle distribution may be resulted from the inhomogeneous mixing during

Table 1
Elemental analysis of HA-Hp microgels.

Samples	C (wt%)	H (wt%)	S (wt%)	Heparin content[a] (wt%)	Heparin conjugation[b] (%)
Heparin	25.02	3.78	10.2	100	–
HA-Hp-1%	35.56	3.96	0.09	0.9	90
HA-Hp-5%	34.23	4.56	0.44	4.6	92
HA-Hp-10%	33.44	4.97	0.91	8.9	89

[a] The actual heparin content in HA-Hp microgels was calculated by the ratio of the sulfur element percentage in HA-Hp microgels and heparin.
[b] The heparin conjugation percentage was evaluated using the ratio of actual and feed content of heparin in HA-Hp microgels.

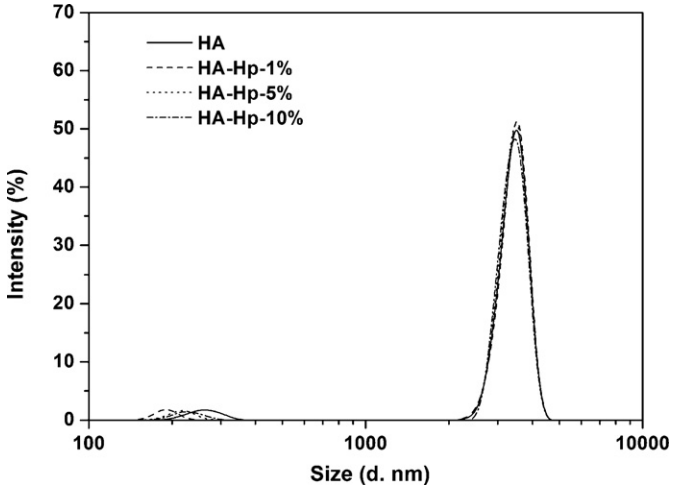

Fig. 3. Particle size and distribution of HA and HA-Hp microgels with different Hp content by DLS analysis.

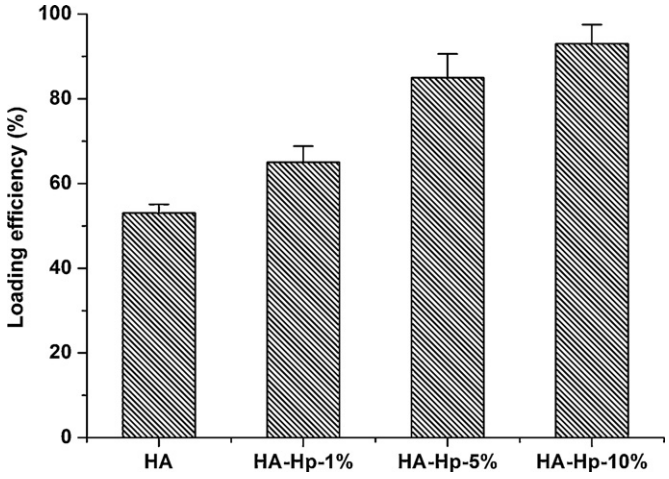

Fig. 5. BMP-2 loading efficiency of HA and HA-Hp microgels with different Hp content. Data points represent mean ± standard deviation, $n = 3$.

the microgel synthesis as well as the inherent polydispersity of an AOT microemulsion system (Kotlarchyk, Chen, & Huang, 1982).

3.5. Equilibrium swelling ratio

Swelling has a significant influence on the solute diffusion, surface properties and mechanical stability of a hydrogel, which depends on the cross-linking density and internal structure of a hydrogel matrix. Swelling ratio, evaluating the cross-linking density and water adsorption capability of a hydrogel network, is an important parameter of a hydrogel in biomedical application (Lin, Tan, Marra, Jan, & Liu, 2009; Zhang, Wang, & Wang, 2010). The equilibrium swelling ratio of HA and various HA-Hp microgels in PBS (pH 7.4) were shown in Fig. 4. Among these samples, HA microgels presented the lowest equilibrium swelling ratio of 9.0, and the equilibrium swelling ratio of HA-Hp microgels got increased by enhancing the heparin content with a maximum value of 11.8 at a heparin level of 10% (w/w). The significant difference in equilibrium swelling ratio should be resulted from the very different interior structure of these four microgel samples with different heparin amount. The lowest swelling ratio of HA microgel was due to its densest network. With the increase of heparin content, the formation of more defects within HA-Hp microgels generated looser internal cross-linking network, which led to the higher water adsorption. Therefore, the highest equilibrium swelling ratio of HA-Hp-10% microgels was attributed to its least dense network, which was confirmed by the SEM and TEM analyses.

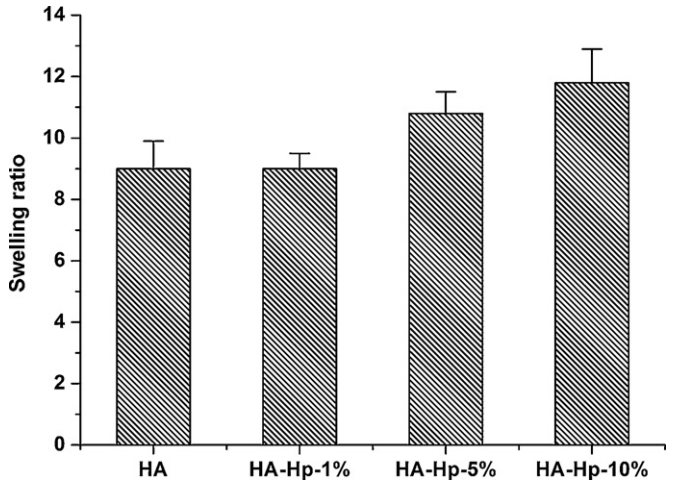

Fig. 4. Equilibrium swelling ratio of HA and HA-Hp microgels with different Hp content in PBS at pH 7.4. Data points represent mean ± standard deviation, $n = 3$.

3.6. BMP-2 loading and release

Both a high protein loading efficiency and a controllable release profile are necessary for biomedical application. Here, the BMP-2 loading efficiency of HA and HA-Hp microgels was analyzed by ELISA in Fig. 5. HA microgels showed a lower BMP-2 loading efficiency of 53% than HA-Hp microgels. Moreover, the BMP-2 loading efficiency of HA-Hp microgels was increased by raising the heparin content and a BMP-2 encapsulation efficiency of over 90% was obtained at 10% (w/w) of heparin. These results implied that the presence of heparin in HA-Hp microgels facilitated BMP-2 binding and led to a higher BMP-2 loading efficiency in comparison with HA microgels. It was possibly due to the electrostatic interaction between basic heparin-binding domain on BMP-2 and acidic sulfate groups on heparin molecules (Yoon, Chung, Lee, & Park, 2006).

Beside a high loading efficiency, a delivery profile of BMP-2 in a controlled manner is another key factor in tissue engineering, which plays a vital role on prolonging the half-life and retaining the bioactivity of BMP-2 (Johnson, Lee, Bellamkonda, & Guldberg, 2009). Fig. 6 shows the cumulative release profiles of BMP-2 from HA and HA-Hp microgels. In comparison to HA-Hp microgels, HA microgels exhibited a faster release rate with a delivery amount of 26% at 1 day, but it was already much slower than that of traditional bulk hydrogel delivery system by physical entrapping protein within matrix (Leach & Schmidt, 2005). This is because the microgel system can prevent the burst release of biomacromolecules that usually takes place in the physically entrapped bulk gel system (Tayalia & Mooney, 2009). It was notable that the release profile of BMP-2 distinctly slowed down during the whole delivery period by conjugating heparin into the microgels. Furthermore, HA-Hp microgels with a higher heparin percentage gave a slower delivery profile. For example, HA-Hp-10% microgels showed the lowest release profile in spite of its highest equilibrium swelling ratio and lowest cross-linking density that favored BMP-2 diffusion. It was seen that only 7% of loaded BMP-2 was released at 1 d, and there were still more than 60% of loaded BMP-2 remaining in the microgel matrix over a long delivery period of 15 days. These results suggested that increasing the heparin content could facilitate the immobilization of BMP-2 and decrease the delivery rate. It might be the reason that the electrostatic attraction between N- and O-

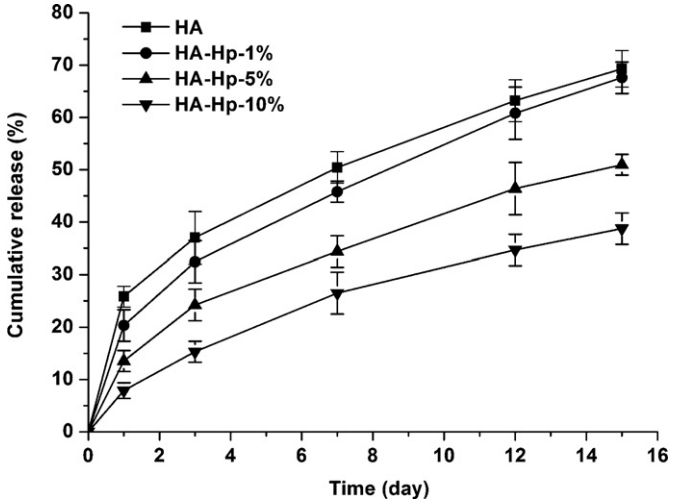

Fig. 6. BMP-2 release profiles from HA and HA-Hp microgels with different Hp content. Data points represent mean ± standard deviation, $n = 3$.

sulfated residues of heparin and the lysine and arginine residues of BMP-2 prevented it from rapid release (Pike et al., 2006). Therefore, a sustained long-term release profile of BMP-2 can be realized by using a HA-Hp microgels delivery system.

4. Conclusion

To develop a controlled GFs delivery system for tissue engineering, a series of heparin-conjugated HA microgels, i.e. HA-Hp microgels, with different heparin content were synthesized using an inverse emulsion polymerization technique. For HA-Hp microgels, heparin was efficiently conjugated to hyaluronan with a conjugation percentage of about 90%. Heparin had little effect on the microgel size, whereas the surface and internal structure were significantly influenced by the heparin content. Rougher surface with holes and concaves, and looser internal structure were generated with increasing the heparin percentage, as opposed to the smooth surface and dense cross-linking network of HA microgels. For this reason, HA-Hp microgels showed a higher equilibrium swelling ratio proportional to the heparin amount than HA microgels. In addition, HA-Hp microgels with a higher heparin content also presented a higher BMP-2 loading efficiency and a slower release profile, which should be attributed to the electrostatic interaction between heparin-binding domain on BMP-2 and acidic sulfate groups on heparin. The long-term sustained release of BMP-2 could be controlled by HA-Hp microgels via regulating the heparin content. Hence, HA-Hp microgels will be a promising controlled delivery system of GFs for tissue engineering.

Acknowledgements

The authors are thankful to financial support from the National Natural Science Foundation of China (No. 30900296).

References

Babensee, J. E., McIntire, L. V., & Mikos, A. G. (2000). Growth factor delivery for tissue engineering. *Pharmaceutical Research*, *17*, 497–504.
Chen, F. M., Wu, Z. F., Sun, H. H., Wu, H., Xin, S. N., Wang, Q. T., et al. (2006). Release of bioactive BMP from dextran-derived microspheres: A novel delivery concept. *International Journal of Pharmaceutics*, *307*, 23–32.
Edelman, E. R., Nugent, M. A., Smith, L. T., & Karnovsky, M. J. (1992). Basic fibroblast growth factor enhances the coupling of intimal hyperplasia and proliferation of vasa vasorum in injured rat arteries. *Journal of Clinical Investigation*, *89*, 465–473.
Godspodarowicz, D., & Cheng, J. (1986). Heparin protects basic and acidic FGF from inactivation. *Journal of Cellular Physiology*, *128*, 475–484.
Goldring, M. B., Tsuchimochi, K., & Ijiri, K. (2006). The control of chondrogenesis. *Journal of Cellular Biochemistry*, *97*, 33–44.
Hahn, S. K., Jelacic, S., Maier, R. V., Stayton, P. S., & Hoffman, A. S. (2004). Anti-inflammatory drug delivery from hyaluronic acid hydrogels. *Journal of Biomaterials Science Polymer Edition*, *15*, 1111–1119.
Hall, B. K., & Miyake, T. (2000). All for one and one for all: Condensations and the initiation of skeletal development. *Bioessays*, *22*, 138–147.
Ho, Y. C., Mi, F. L., Sung, H. W., & Kuo, P. L. (2009). Heparin-functionalized chitosan-alginate scaffolds for controlled release of growth factor. *International Journal of Pharmaceutics*, *376*, 69–75.
Jha, A. K., Hule, R. A., Jiao, T., Teller, S. S., Clifton, R. J., Duncan, R. L., et al. (2009). Structural analysis and mechanical characterization of hyaluronic acid-based doubly cross-linked networks. *Macromolecules*, *42*, 537–546.
Jiang, D., Liang, J., & Noble, P. W. (2007). Hyaluronan in tissue injury and repair. *Annual Review of Cell and Developmental Biology*, *23*, 435–461.
Johnson, M. R., Lee, H. J., Bellamkonda, R. V., & Guldberg, R. E. (2009). Sustained release of BMP-2 in a lipid-based microtube vehicle. *Acta Biomaterialia*, *5*, 23–28.
Kotlarchyk, M., Chen, S. H., & Huang, J. S. (1982). Temperature dependence of size and polydispersity in a three-component microemulsion by small-angle neutron scattering. *Journal of Physics and Chemistry*, *86*, 3273–3276.
Krawczak, D. A., Westendorf, J. J., Carlson, C. S., & Lewis, J. L. (2009). Influence of bone morphogenetic protein-2 on the extracellular matrix, material properties, and gene expression of long-term articular chondrocyte cultures: Loss of chondrocyte stability. *Tissue Engineering Part A*, *15*, 1247–1255.
Leach, J. B., & Schmidt, C. E. (2005). Characterization of protein release from photocrosslinkable hyaluronic acid-polyethylene glycol hydrogel tissue engineering scaffolds. *Biomaterials*, *26*, 125–135.
Liao, I. C., Wan, A. C. A., Yim, E. K. F., & Leong, K. M. (2005). Controlled release from fibers of polyelectrolyte complexes. *Journal of Controlled Release*, *104*, 347–358.
Lin, Y. C., Tan, F. J., Marra, K. G., Jan, S. S., & Liu, D. C. (2009). Synthesis and characterization of collagen/hyaluronan/chitosan composite sponges for potential biomedical applications. *Acta Biomaterialia*, *5*, 2591–2600.
Lou, X., Vijayasekaran, S., Sugiharti, R., & Robertson, T. (2005). Morphological and topographic effects on calcification tendency of pHEMA hydrogels. *Biomaterials*, *26*, 5808–5817.
Maeda, H., Sano, A., & Fujioka, K. (2004). Controlled release of rhBMP-2 from collagen minipellet and the relationship between release profile and ectopic bone formation. *International Journal of Pharmaceutics*, *275*, 109–122.
Nakamura, S., Nambu, M., Ishizuka, T., Hattori, H., Kanatani, Y., Takase, B., et al. (2007). Effect of controlled release of fibroblast growth factor-2 from chitosan/fucoidan micro complex-hydrogel on in vitro and in vivo vascularization. *Journal of Biomedical Materials Research*, *85A*, 619–627.
Nimni, M. E. (1997). Polypeptide growth factors: Targeted delivery systems. *Biomaterials*, *18*, 1201–1215.
Oh, J. K., Lee, D. I., & Park, J. M. (2009). Biopolymer-based microgels/nanogels for drug delivery applications. *Progress in Polymer Science*, *34*, 1261–1282.
Pike, D. B., Cai, S. S., Pomraning, K. R., Firpo, M. A., Fisher, R. J., Shu, X. Z., et al. (2006). Heparin-regulated release of growth factors in vitro and angiogenic response in vivo to implanted hyaluronan hydrogels containing VEGF and bFGF. *Biomaterials*, *27*, 5242–5251.
Rizzi, S. C., Ehrbar, M., Halstenberg, S., Raeber, G. P., Schmoekel, H. G., Hagenmuller, H., et al. (2006). Recombinant protein-co-PEG networks as cell-adhesive and proteolytically degradable hydrogel matrixes. Part II. Biofunctional characteristics. *Biomacromolecules*, *7*, 3019–3029.
Sahoo, S., Chung, C., Khetan, S., & Burdick, J. A. (2008). Hydrolytically degradable hyaluronic acid hydrogels with controlled temporal structures. *Biomacromolecules*, *9*, 1088–1092.
Tayalia, P., & Mooney, D. J. (2009). Controlled growth factor delivery for tissue engineering. *Advanced Materials*, *21*, 3269–3285.
Toole, B. P. (2001). Hyaluronan in morphogenesis. *Seminars in Cell and Developmental Biology*, *12*, 79–87.
Wissink, M. J. B., Beernink, R., Poot, A. A., Engbers, G. H. M., Beugeling, T., van Aken, W. G., et al. (2000). Improved endothelialization of vascular grafts by local release of growth factor from heparinized collagen matrices. *Journal of Controlled Release*, *64*, 103–114.
Yang, X., & Kim, J. C. (2010). Novel pH-sensitive microgels prepared using salt bridge. *International Journal of Pharmaceutics*, *388*, 58–63.
Yoon, J. J., Chung, H. J., Lee, H. J., & Park, T. G. (2006). Heparin-immobilized biodegradable scaffolds for local and sustained release of angiogenic growth factor. *Journal of Biomedical Materials Research*, *79A*, 934–942.
Zavan, B., Vindigni, V., Vezzù, K., Zorzato, G., Luni, C., Abatangelo, G., et al. (2009). Hyaluronan based porous nano-particles enriched with growth factors for the treatment of ulcers: A placebo-controlled study. *Journal of Materials Science: Materials in Medicine*, *20*, 235–247.
Zeng, R., Tu, M., Liu, H. W., Zhao, J. H., Zha, Z. G., & Zhou, C. R. (2009). Preparation, structure, drug release and bioinspired mineralization of chitosan-based nanocomplexes for bone tissue engineering. *Carbohydrate Polymers*, *78*, 107–111.
Zhang, J., Wang, Q., & Wang, A. (2010). In situ generation of sodium alginate/hydroxyapatite nanocomposite beads as drug-controlled release matrices. *Acta Biomaterialia*, *6*, 445–454.
Zhao, J. H., Han, W. Q., Chen, H. D., Tu, M., Zeng, R., Shi, Y. F., et al. (2011). Preparation, structure and crystallinity of chitosan nano-fibers by a solid-liquid phase separation technique. *Carbohydrate Polymers*, *83*, 1541–1546.